

การเคลือบด้วยลำโม่เลกุลและการหาลักษณะเฉพาะของชั้นคอปเปอร์อินเดียมแกลเลียมไดซีลีไนต์
ที่มีช่องว่างแถบพลังงานกว้างสำหรับเซลล์แสงอาทิตย์ชนิดฟิล์มบาง

นางสาวปณิตา ชินเวชกิจวานิชย์

วิทยานิพนธ์นี้เป็นส่วนหนึ่งของการศึกษาตามหลักสูตรปริญญาวิทยาศาสตรดุษฎีบัณฑิต

สาขาวิชาฟิสิกส์ ภาควิชาฟิสิกส์

คณะวิทยาศาสตร์ จุฬาลงกรณ์มหาวิทยาลัย

ปีการศึกษา 2549

ISBN 974-14-2988-6

ลิขสิทธิ์ของจุฬาลงกรณ์มหาวิทยาลัย

MOLECULAR BEAM DEPOSITION AND CHARACTERIZATION
OF WIDE-BAND-GAP $\text{Cu}(\text{In,Ga})\text{Se}_2$ FOR THIN FILM SOLAR CELLS

Miss. Panita Chinvetkitvanich

A Dissertation Submitted in Partial Fulfillment of the Requirements
for the Degree of Doctor of Philosophy Program in Physics

Department of Physics

Faculty of Science

Chulalongkorn University

Academic Year 2006

ISBN 974-14-2988-6

Copyright of Chulalongkorn University

492239


Thesis Title MOLECULAR BEAM DEPOSITION AND
CHARACTERIZATION OF WIDE-BAND-GAP
Cu(In,Ga)Se₂ FOR THIN FILM SOLAR CELLS
By Miss. Panita Chinvetkitvanich
Field of Study Physics
Thesis Advisor Assistant Professor Kajornyod Yoodee, Ph.D.
Thesis Co-advisor Assistant Professor Somphong Chatraphorn

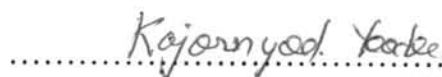
Accepted by the Faculty of Science, Chulalongkorn University in Partial
Fulfillment of the Requirements of the Doctoral Degree




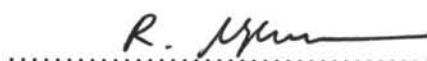
..... Dean of the Faculty of Science
(Professor Piamsak Menasveta, Ph.D.)


THESIS COMMITTEE

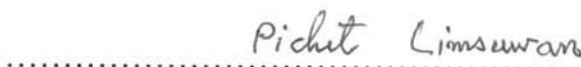
..... Chairman
(Assistant Professor Piamsak Ratanavararak, Ph.D.)

..... Thesis Advisor
(Assistant Professor Kajornyod Yoodee, Ph.D.)

..... Thesis Co-advisor
(Assistant Professor Somphong Chatraphorn)

..... Member
(Assistant Professor Rattachat Mongkolnavin, Ph.D.)

..... Member
(Chatchai Srinitiwatwong, Ph.D.)

..... Member
(Associate Professor Pichet Limsuwan, Ph.D.)

ปณิตา ชินเวชกิจวานิชย์ : การเคลือบด้วยลำโมเลกุลและการหาลักษณะเฉพาะของชั้นคอปเปอร์อินเดียมแกลเลียมไดซีสไนด์ที่มีช่องว่างแถบพลังงานกว้างสำหรับเซลล์แสงอาทิตย์ชนิดฟิล์มบาง. (MOLECULAR BEAM DEPOSITION AND CHARACTERIZATION OF WIDE-BAND-GAP $\text{Cu}(\text{In,Ga})\text{Se}_2$ FOR THIN FILM SOLAR CELLS) อ. ที่ปรึกษา : ผศ. ดร. ขจรยศ อยุดี, อ. ที่ปรึกษาร่วม : ผศ. สมพงษ์ ฉัตรภรณ์, 162 หน้า. ISBN 974-14-2988-6

ได้เตรียมฟิล์มบางพหุผลึก $\text{CuIn}_{1-x}\text{Ga}_x\text{Se}_2$ ($\text{Cu}(\text{In,Ga})\text{Se}_2$) โดยวิธีการเคลือบด้วยลำโมเลกุล (MBD) ร่วมกับการใช้เทคนิคการตรวจวัดสัญญาณ ณ เวลาจริง เพื่อให้ควบคุมกระบวนการและที่จุดสิ้นสุด (EPD) ในการทดลองเตรียมฟิล์มบาง $\text{Cu}(\text{In,Ga})\text{Se}_2$ ได้ใช้โปรไฟล์อุณหภูมิ 2 แบบ โดยแบบแรกคือ two-stage process เริ่มต้นจาก Cu-rich stage ด้วยการปลูกให้ฟิล์มมีสัดส่วนอะตอมของ $[\text{Cu}]/([\text{In}]+[\text{Ga}])$ มากกว่าหนึ่ง ($y > 1$) แล้วต่อด้วย Cu-poor stage จนกระทั่งได้เนื้อฟิล์มทั้งหมดที่มีค่า $y < 1$ และหยุดปลูกที่ค่า $y \approx 0.9$ ทั้งนี้ได้เตรียมฟิล์มบาง $\text{CuIn}_{1-x}\text{Ga}_x\text{Se}_2$ ที่แปรค่า x ตั้งแต่ 0 ถึง 1 และได้เตรียมฟิล์มบาง CuGaSe_2 ที่แปรค่า y จาก 1.45 ถึง 0.7 จากผลการวิเคราะห์ฟิล์มด้วยวิธี XRD และ SEM พบว่าฟิล์มที่เตรียมด้วยวิธี MBD แบบนี้มีโครงสร้างแบบซาลโคไฟไรท์ โดยโครงสร้างชั้นระนาบ (112) ขนานกับระนาบของแผ่นรองรับเป็นจำนวนมาก มีเกรนเป็นแท่งใหญ่และผิวขรุขระมีรอยแตกแยกเล็ก จากผลการวัดลักษณะเฉพาะของกระแสและความต่างศักย์ไฟฟ้า (I-V) พบว่าเซลล์แสงอาทิตย์ของฟิล์ม $\text{CuIn}_{1-x}\text{Ga}_x\text{Se}_2$ ที่เตรียมแบบ two-stage process นี้มีประสิทธิภาพสูงถึง 11% (ที่ค่า $x=0.3$) และประสิทธิภาพของเซลล์มีค่าลดลงเมื่อ $x \geq 0.5$ ส่วนโปรไฟล์แบบที่สอง three-stage process เริ่มต้นปลูกชั้น $(\text{In,Ga})_2\text{Se}_3$ precursor มีค่า $y=0$ แล้วต่อด้วย Cu-rich stage จนกระทั่งได้เนื้อฟิล์มมีค่า $y > 1$ แล้วต่อด้วย Cu-poor stage จนกระทั่งได้เนื้อฟิล์มที่มีค่า $y \approx 0.9$ จากผลการวิเคราะห์ด้วยวิธี XRD และ SEM พบว่าฟิล์มที่เตรียมด้วยวิธี MBD แบบนี้มีโครงสร้างแบบซาลโคไฟไรท์ โครงสร้างชั้นระนาบ (112) ขนานกับระนาบของแผ่นรองรับเป็นจำนวนน้อยกว่าแบบแรก มีเกรนเป็นแท่งและผิวเรียบมีรอยแตกแยกที่ไม่ลึก ทั้งนี้พบว่ามี recrystallization จากชั้นอัญฐาน $(\text{In,Ga})_2\text{Se}_3$ precursor ไปเป็นพหุผลึก $\text{Cu}(\text{In,Ga})\text{Se}_2$ ที่มีโครงสร้างแบบซาลโคไฟไรท์ ซึ่งคาดว่าเป็นจุดเริ่มต้นของเฟสซาลโคไฟไรท์ที่เสถียร สำหรับเซลล์แสงอาทิตย์ของฟิล์ม $\text{Cu}(\text{In,Ga})\text{Se}_2$ ที่เตรียมแบบ three-stage process นี้ได้ค่าประสิทธิภาพที่สูงถึง 15.3% (ที่ค่า $x=0.3$) อีกทั้งจากผลการวิเคราะห์เชิงแสงของฟิล์ม CuGaSe_2 ที่แปรค่า y จาก 1.45 ถึง 0.7 ซึ่งเตรียมด้วยวิธี MBD นี้ ยังพบว่ามีคุณภาพสูงในระดับ excitonic grade อีกด้วย

ภาควิชา ฟิสิกส์
สาขาวิชา ฟิสิกส์
ปีการศึกษา 2549

ลายมือชื่อนิติ.....
ลายมือชื่ออาจารย์ที่ปรึกษา.....
ลายมือชื่ออาจารย์ที่ปรึกษาร่วม.....

4473862123 : MAJOR PHYSICS

KEY WORD: SOLAR CELL / FABRICATION / IN SITU MONITORING / WIDE-BAND-GAP/ $\text{CuIn}_{1-x}\text{Ga}_x\text{Se}_2$

PANITA CHINVETKITVANICH: MOLECULAR BEAM DEPOSITION AND CHARACTERIZATION OF WIDE-BAND-GAP $\text{Cu}(\text{In,Ga})\text{Se}_2$ FOR THIN FILM SOLAR CELLS. THESIS ADVISOR: ASST. PROF. KAJORNYOD YOODEE, PH.D., THESIS COADVISOR: ASST. PROF. SOMPHONG CHATRAPHORN. 162 pp. ISBN 974-14-2988-6

$\text{CuIn}_{1-x}\text{Ga}_x\text{Se}_2$: $\text{Cu}(\text{In,Ga})\text{Se}_2$ polycrystalline thin films were prepared by the molecular beam deposition (MBD) method. The *in situ* monitoring technique was employed for process control and end-point detection (EPD). Two temperature profiles were performed in the $\text{Cu}(\text{In,Ga})\text{Se}_2$ deposition process. First, the two-stage growth process was started with the Cu-rich stage such that the atomic ratio $y=[\text{Cu}]/([\text{In}]+[\text{Ga}])$ was greater than 1.0 ($y>1$), then followed by the Cu-poor stage until $y<1$ was reached, and the process was finished at $y\approx 0.9$. Using this technique, the $\text{CuIn}_{1-x}\text{Ga}_x\text{Se}_2$ thin films of varied x from 0 to 1 and the CuGaSe_2 films of varied y from 1.45 to 0.7 were fabricated. The XRD and SEM results showed that all MBD polycrystalline CuGaSe_2 films were strongly (112) oriented chalcopyrite with large columnar grains and rough surfaces with deep crevices. From the current-voltage (I-V) measurement, the $\text{Cu}(\text{In,Ga})\text{Se}_2$ thin film solar cells fabricated with two-stage growth process yielded efficiencies 11% ($x=0.3$) and the efficiencies decrease for wide band gap $\text{Cu}(\text{In,Ga})\text{Se}_2$ ($x\geq 0.5$) film. The second profile, three-stage growth process, started with $(\text{In,Ga})_2\text{Se}_3$ precursor, $y=0$, followed by the Cu-rich stage until $y>1$, then finished with the Cu-poor stage at $y\approx 0.9$. The XRD and SEM results of the grown films using this process showed weakly (112) oriented chalcopyrite with columnar grains and smooth surfaces with shallow crevices. The evidence of recrystallization from amorphous- $(\text{In,Ga})_2\text{Se}_3$ precursor to polycrystalline $\text{Cu}(\text{In,Ga})\text{Se}_2$ chalcopyrite structure was also observed and expected to be the origin of the stabilized $\text{Cu}(\text{In,Ga})\text{Se}_2$ chalcopyrite phase. The $\text{Cu}(\text{In,Ga})\text{Se}_2$ thin film solar cells fabricated using the three-stage growth process showed the efficiency up to 15.3% ($x=0.3$). The cell performances of the wide band gap $\text{Cu}(\text{In,Ga})\text{Se}_2$ solar cells also improved using the three-stage growth process. Moreover, the optical characterization of CuGaSe_2 thin films revealed that the high quality with excitonic grade CuGaSe_2 polycrystalline thin films in a wide range of y from 1.45 to 0.70 could be fabricated by MBD method.

Department Physics
Field of Study Physics
Academic Year 2006

Student's Signature.....*Panita Chinvetkitvanich*
Advisor's Signature.....*Kajornyod Yodee*
Co-advisor's Signature.....*Somphong Chatraphorn*

Acknowledgements

I would like to express my sincere gratitude and appreciation to my thesis advisors, Assistant Professor Dr. Kajornyod Yoodee and Assistant Professor Somphong Chatraphorn for their supervision, invaluable discussion, scientific skill, kindness suggestion and advice throughout the course of this thesis.

I would like to grateful to Assistant Professor Dr. Pisistha Ratanavararak, Assistant Professor Dr. Rattachat Mongkolnavin, Dr. Chatchai Srinitiwarawong and Associate Professor Dr. Pichet Limsuwan for serving as a chairman and committee, respectively. All of whom have made valuable comments and have been helpful in the production of this thesis.

I especially would like to thank to Dr. Chanwit Chityuttakan for many helpful discussions, new and interesting ideas, scientific knowledge, technical supports, and encouragement throughout the period of my graduate studies. I also would like to thanks Assistant Professor Dr. Sojiphong Chatraphorn for technical supports, especially AFM characterization, and thank to Mr. Rachsak Sakdanupab for his help in solar cell fabrication process.

Many thanks to my colleagues in Semiconductor Physics Research Laboratory, Department of Physics, Chulalongkorn University, for their friendship and help me in various way.

I would like to acknowledge the financial support from the Department of Physics, King Mongkutt's University of Technology Thonburi for the scholarship for my study. I also would like to acknowledge the assistantship granted by the National Research Council.

Finally, a deep gratitude is acknowledged to my family, for understanding, encouragement throughout the entire study and everything they have done for me.

Contents

Abstract (Thai).....	iv
Abstract (English).....	v
Acknowledgements.....	vi
List of Tables.....	xi
List of Figures.....	xiii
1. Introduction.....	1
1.1 Overview.....	1
1.2 Types of Solar Cells.....	2
1.2.1 Single-crystalline and Polycrystalline Silicon.....	2
1.2.2 III-V Group Single Crystals.....	3
1.2.3 Thin Film Solar Cells.....	3
1.3 Motivation of the Research.....	6
1.4 Objectives of the Research.....	7
1.5 Thesis Organization.....	7
2. Theoretical Background.....	9
2.1 Material Properties of $\text{CuIn}_{1-x}\text{Ga}_x\text{Se}_2$ Chalcopyrite Semiconductors	9
2.1.1 Phase Diagram of Cu-In-Se System.....	10
2.1.2 Phase Diagram of Cu-Ga-Se System.....	12
2.2 Defects in CuInSe_2	13
2.3 Band Gap Engineering of Ternary Chalcopyrite Semiconductors.....	15
2.4 Principle of Solar Cells.....	17
2.4.1 Solar Spectrum.....	17
2.4.2 Electrical Properties of Solar Cells.....	18
2.4.3 Current-Voltage Characteristics.....	20
2.4.4 Efficiency Limits.....	23

3. Molecular Beam Deposition.....	26
3.1 Overview of Molecular Beam Epitaxy	26
3.2 Basic Physical Mechanism of MBE Growth.....	27
3.3 The Molecular Beam Epitaxy (MBE) System.....	28
3.3.1 The Main Growth Chamber.....	29
3.3.2 The Load Lock Chamber.....	31
3.3.3 <i>In situ</i> Diagnostic Techniques.....	31
3.3.3.1 Beam Flux Monitor (BFM).....	31
3.3.3.2 Residual Gas Analyzer (RGA).....	32
3.3.3.3 Quartz Crystal Thickness Monitor (QCM).....	32
3.3.3.4 Reflection High Energy Electron Diffraction (RHEED).....	33
3.3.3.5 Pyrometer.....	36
3.4 System Preparation and Characterization.....	37
3.4.1 Baking the MBE System.....	37
3.4.2 Checking the Residual Gas Using the RGA.....	38
3.4.3 Outgassing of Crucibles and Source Materials.....	40
3.5 Calibration of Growth Parameters.....	41
3.5.1 Substrate Cleaning Procedure.....	41
3.5.1.1 Soda-lime Glass Cleaning Procedure.....	41
3.5.1.2 GaAs Wafer Cleaning Procedure.....	42
3.5.2 Calibration of Substrate Temperature.....	43
3.5.3 Calibration of Effusion Cells.....	48
3.6 Conclusions.....	55
4. Experimental Methods	56
4.1 Fabrication of Ni-Al/ZnO/i-ZnO/CdS/CuIn _{1-x} Ga _x Se ₂ /Mo/SLG Thin Film Solar Cells.....	56
4.1.1 Substrate Preparation.....	58

4.1.2	Molybdenum Back Contact Preparation.....	59
4.1.3	Cu(In,Ga)Se ₂ Absorber Layer Preparation.....	59
4.1.4	Cadmium Sulfide Buffer Layer Preparation.....	60
4.1.5	ZnO(Al)/i-ZnO Window Bi-layer Preparation.....	61
4.1.6	Ni-Al Grid Front Contact Preparation.....	61
4.2	Preparation of Cu(In,Ga)Se ₂ Thin Films.....	62
4.2.1	Two-stage Growth Process.....	63
4.2.2	Three-stage Growth Process.....	65
4.2.3	<i>In situ</i> Monitoring and End Point Detection Technique.....	67
4.3	Characterization of Cu(In,Ga)Se ₂ Thin Films.....	71
4.3.1	Structural Analysis.....	71
4.3.2	Transmittance and Reflectance Measurements.....	76
4.3.3	Current-Voltage (I-V) Characterization.....	77
5.	Results and Discussion.....	79
5.1	Growth of CuIn _{1-x} Ga _x Se ₂ Thin Films with Variation of x Using Two-stage Growth Process.....	79
5.1.1	<i>In situ</i> Signals and Film Characterization.....	79
5.1.2	Evaluation of Optical Parameters.....	83
5.2	Evolution of Structural and Morphology of CuGaSe ₂ Thin Films Grown by MBD Using Two-stage Growth Process.....	90
5.3	Growth and Characterization of CuGaSe ₂ Thin Films Grown by MBD Using Three-stage Growth Process.....	102
5.3.1	<i>In situ</i> Monitoring Signals of the Growth of CuGaSe ₂ Thin Films Using Three-stage Process.....	102
5.3.2	Evolution of Crystal Structure of the CuGaSe ₂ Films Grown by Three -stage Process.....	105
5.3.3	Morphology and Grain Growth of the CuGaSe ₂ Films Grown	

by Three -stage Process.....	109
5.4 Solar Cell Devices Analysis.....	111
5.4.1 CuIn _{1-x} Ga _x Se ₂ –Based Thin Film Solar Cells: Absorber Grown by Two-stage Growth Process	112
5.4.2 CuIn _{1-x} Ga _x Se ₂ –Based Thin Film Solar Cells: Absorber Grown by Three-stage Growth Process	114
5.4.3 Comparison of Cell Performances of the CuIn _{1-x} Ga _x Se ₂ Thin Film Solar Cells Grown by Two-stage versus Three-Stage Growth Processes	117
6. Conclusions and Suggestions.....	121
References.....	124
Appendices.....	132
Appendix A List of Symbols and Abbreviations.....	133
Appendix B General Calculation for CuIn _{1-x} Ga _x Se ₂ Deposition Process..	138
Appendix C List of Publications.....	142
Vitae.....	145

List of Tables

2.1	Majority defect pairs in CuInSe_2 under the condition $\Delta m < 0$	14
2.2	Formation energies of intrinsic defects in CuInSe_2	14
3.1	List of possible species of gases found in the MBE chamber detected by a RGA. Some species are decomposed from stable gas molecules	39
3.2	Flux conversion factor for source elements	50
3.3	Calibration of the Cu effusion cell	51
3.4	Calibration of the In effusion cell	52
3.5	Calibration of the Ga effusion cell	53
3.6	Calibration of the Se effusion cell	54
4.1	Typical chemical composition of the soda-lime glass substrates.....	58
5.1	Chemical composition of representative $\text{CuIn}_{1-x}\text{Ga}_x\text{Se}_2$ films	81
5.2	The calculation of n at maxima, minima wavelengths of $\text{CuIn}_{1-x}\text{Ga}_x\text{Se}_2$ film with $x = 0.50$ and thickness of $2.213 \mu\text{m}$	85
5.3	A and B values for $\text{CuIn}_{1-x}\text{Ga}_x\text{Se}_2$ films with Ga contents of $x=0.00$, $x=0.35$, $x=0.50$, $x=0.70$, $x=0.80$, and $x=1.00$	87
5.4	Calculated values of a, c, c/a and z from the XRD patterns of the films R, S and P shown in Fig. 5.10 and JCPDS of CuGaSe_2	93
5.5	Summary of the chemical composition of representative CuGaSe_2 films presented in Fig 5.9.....	94
5.6	Summary of the chemical composition of representative CuGaSe_2 films presented in Fig. 5.16.....	105
5.7	Calculated values of a, c, c/a and z from the XRD patterns of the films N, Q, R and S shown in Fig. 5.17 and JCPDS of CuGaSe_2	108
5.8	The average photovoltaic parameters of $\text{CuIn}_{1-x}\text{Ga}_x\text{Se}_2$ thin film solar cells with various x of absorber layers grown by two-stage process	112

5.9	The average photovoltaic parameters of $\text{CuIn}_{1-x}\text{Ga}_x\text{Se}_2$ thin film solar cells with various x of absorber layers grown by three-stage process	114
-----	---	-----

List of Figures

1.1	Absorption coefficient spectrum of CuInSe_2 compared with that of other photovoltaic semiconductors	6
2.1	Schematic representation of CuInSe_2 chalcopyrite structure analogs to ZnSe zinc blende structure	10
2.2	$\text{Cu}_2\text{Se-In}_2\text{Se}_3$ pseudo-binary phase diagram.....	12
2.3	Phase diagram along the $\text{Cu}_2\text{Se-Ga}_2\text{Se}_3$ pseudo-binary section of the Cu-Ga-Se material system	13
2.4	Band structure of chalcopyrite type semiconductor (a) CuGaSe_2 and (b) CuInSe_2 . The indications \perp and \parallel show that the transition is allowed for the light polarization E perpendicular and parallel to the crystal axis, respectively. The value Δ_{so} and Δ_{cf} are the spin-orbit and crystal field splittings, respectively	16
2.5	Spectral distribution of sunlight. The dashed line indicates the radiation distribution expected from the sun if it were a black body at a temperature of 6000K.....	18
2.6	A simplified energy band diagram of p-n heterojunction solar cell (a) at thermal equilibrium in dark (b) under forward bias (c) under a reverse bias and (d) under illumination, open circuit conditions. No 1 and 2 in the Figure refer n-type and p-type semiconductor, respectively.....	19
2.7	I-V characteristic curves.....	21
2.8	Equivalent circuit of p-n junction solar cells.....	22
2.9	Upper limits of the short-circuit current density as a function of the energy band gap of the solar cell material.....	23
2.10	Theoretical solar cell efficiency as a function of band gap for spectrum distribution at AM1.5 and AM0 with a power density of 1 sun, and for AM1.5	

	with 1000 sun (= 844 kW/m ²).....	25
2.11	The major loss mechanism in solar cells.....	25
3.1	EW100 MBE system installed at the SPRL, Chulalongkorn University.....	29
3.2	A schematic diagram of a RHEED measurement. The array of rods is the reciprocal lattice rods. Diffracted beams have maximum intensities when the Ewald sphere cuts the rods.....	34
3.3	A plan view showing the relation between the intra row spacing of the reciprocal lattice rods and the spacing of the observed RHEED streaks.....	35
3.4	RHEED patterns from surfaces with different morphologies.....	36
3.5	Pressure in the main growth chamber before and after baking process.....	38
3.6	Mass/Charge spectrum obtained from the RGA at $P \approx 3 \times 10^{-10}$ Torr.....	38
3.7	RHEED patterns from the GaAs surface (a) at room temperature showing amorphous oxide covering the surface, (b) at 583 °C when the oxide layer is removed from the surface.....	45
3.8	Comparison of the temperature profile reading from pyrometer and the PID controller setting.....	46
3.9	Calibration curve of the surface temperature of SLG versus PID controller setting.....	46
3.10	Schematic diagram of the arrangement of the substrate heater and the position of the pyrometer. The pyrometer was focused on the center of substrate. (A) Typical set-up and (B) modified set-up that the heat diffuser provided paste-free, uniform and reproducible heating of the substrate.....	47
3.11	Time response of the BEP for an In source.....	49
3.12	Time response of the BEP for an Se source.....	49
3.13	Calibration of the Cu effusion cell.....	51
3.14	Calibration of the In effusion cell.....	52
3.15	Calibration of the Ga effusion cell.....	53

3.16	Calibration of the Se effusion cell.....	54
4.1	A schematic representation (not to scale) of Cu(In,Ga)Se ₂ -based thin film solar cell device	57
4.2	Processing steps of fabrication of Cu(In,Ga)Se ₂ -based thin film solar cell	57
4.3	Photograph of Cu(In,Ga)Se ₂ -based thin film solar cells 10 cells fabricated at SPRL	62
4.4	Temperature profiles of two-stage growth process	63
4.5	Evolution of composition in two-stage growth process	65
4.6	Temperature profiles of three-stage growth process	66
4.7	Evolution of composition in three-stage growth process	67
4.8	<i>in situ</i> monitoring signals of the CuIn _{1-x} Ga _x Se ₂ film grown with the two-stage as a function of process time	69
4.9	X-ray spectrum of a Cu(In,Ga)Se ₂ thin film.....	72
4.10	Working principle of the AFM (non contact tapping mode).....	74
4.11	Diffraction of X-rays from parallel planes in the crystal	75
4.12	Typical XRD spectrum of the Cu(In,Ga)Se ₂ thin films.....	76
4.13	Schematic diagram of the I-V measurement system.....	78
5.1	Temperature profiles of elemental sources for two-stage growth process.....	80
5.2	Typical profiles of the <i>in situ</i> signals; T _{Pyro} , OP, and the substrate temperature (TC) during the two-stage growth process of CuIn _{1-x} Ga _x Se ₂ films.....	81
5.3	SEM micrographs of five representative CuIn _{1-x} Ga _x Se ₂ films with x ratios of: (A) 0.0; (B) 0.37; (C) 0.52; (D) 0.69 and (E) 1.0.....	82
5.4	Optical transmittance versus wavelength traces for five representative CuIn _{1-x} Ga _x Se ₂ films having different [Ga]/([In]+[Ga]) ratios. Transmittance spectra of CuIn _{1-x} Ga _x Se ₂ thin films deposited by MBD with Ga contents of x=0.00, x=0.35, x=0.50, x=0.70, x=0.80, and x=1.00.....	84

5.5	Reflection spectrum of $\text{CuIn}_{1-x}\text{Ga}_x\text{Se}_2$ film with $x = 0.5$	86
5.6	Curves of n versus λ , corresponding to $\text{CuIn}_{1-x}\text{Ga}_x\text{Se}_2$ thin film fabricated by MBD with Ga contents of $x=0.00$, $x=0.35$, $x=0.50$, $x=0.70$, $x=0.80$, and $x=1.00$	86
5.7	Example of absorption spectra of $\text{CuIn}_{1-x}\text{Ga}_x\text{Se}_2$ thin films with x -ratios ranging from 0.00 to 1.00 measured at 300K.....	88
5.8	Variation of band gap energy (E_g) with x values of $\text{CuIn}_{1-x}\text{Ga}_x\text{Se}_2$ films.....	89
5.9	Profiles of <i>in situ</i> monitoring signals.....	90
5.10	XRD spectra of the films R , S and P represent the evolution of CuGaSe_2 films grown by two-stage process as shown in Fig. 5.9.....	92
5.11	Surface and cross-section SEM images of CuGaSe_2 films with various Cu/Ga-ratios prepared by two-stage process.....	96
5.12	AFM pictures of selective CuGaSe_2 thin films: film R (Cu/Ga \approx 1.45), film S (Cu/Ga \approx 0.90) and film P (Cu/Ga \approx 0.70).....	99
5.13	Optical absorption spectra of CuGaSe_2 thin films with Cu/Ga-ratio ranging from 1.45 to 0.70 measured at room temperature.....	100
5.14	Typical result of the simplified fitting method for the optical absorption spectrum of CuGaSe_2 thin film (film R).....	101
5.15	Typical temperature profiles of Cu, Ga and Se sources and the substrate temperature (T_{sub}) in the three-stage process of CuGaSe_2 thin film growth..	102
5.16	Typical profiles of the <i>in situ</i> monitoring signals; T_{pyro} and OP during the three-stage process of CuGaSe_2 films.....	103
5.17	XRD spectra of the films N , Q , R and S represent the evolution of CuGaSe_2 films grown by three-stage process as shown in Fig. 5.16.....	106
5.18	Surface and cross-section images of the films N , Q , R and S represent the evolution of film growth during the three-stage process as shown in Fig. 5.16.....	109

5.19	Average photovoltaic parameters of the Ni(Al)/ZnO/i-ZnO/CdS/ CuIn _{1-x} Ga _x Se ₂ /Mo/SLG solar cells with respect to the [Ga]/([In]+[Ga]) ratio based on as-grown CuIn _{1-x} Ga _x Se ₂ absorbers prepared by MBD two- stage process.....	113
5.20	Average photovoltaic parameters of the Ni(Al)/ZnO/i-ZnO/CdS/ CuIn _{1-x} Ga _x Se ₂ /Mo/SLG solar cells with respect to the [Ga]/([In]+[Ga]) ratio based on as-grown CuIn _{1-x} Ga _x Se ₂ absorbers prepared by MBD three- stage process.....	115
5.21	Selected J-V curves with various [Ga]/([In]+[Ga]) of CuIn _{1-x} Ga _x Se ₂ films grown by three-stage process.....	116
5.22	J-V curve of the best CuIn _{1-x} Ga _x Se ₂ solar cell using the <i>in situ</i> monitoring in the three-stage process with x = 0.3.....	117
5.23	Comparison of the average photovoltaic parameters of CuIn _{1-x} Ga _x Se ₂ thin film solar cells with CuIn _{1-x} Ga _x Se ₂ absorber layers grown by two- stage versus three-stage processes.....	118
5.24	Comparison of J-V curves of CuGaSe ₂ thin film solar cells with CuGaSe ₂ absorber layers grown by two-stage versus three-stage processes.....	119